IEEE Access
Multidisciplinary ⋮ Rapid Review ⋮ Open Access Journal

Received 11 January 2024, accepted 29 January 2024, date of publication 6 February 2024, date of current version 20 February 2024.

Digital Object Identifier 10.1109/ACCESS.2024.3362976

RESEARCH ARTICLE

Cooperative Flight Control of a Fleet of Quadrotors Using Fractional Sliding Mode With Potential Field Algorithms

NAJIB ALABSARI[1], ABDUL-WAHID A. SAIF[1,2,3], SAMI EL-FERIK[1,2], SALIH DUFFUAA[2,3], AND NABIL DERBEL[4], (Senior Member, IEEE)

[1]Department of Control and Instrumentation Engineering, King Fahd University of Petroleum and Minerals, Dhahran 31261, Saudi Arabia
[2]Interdisciplinary Research Centre for Smart Mobility and Logistics, King Fahd University of Petroleum and Minerals, Dhahran 31261, Saudi Arabia
[3]Industrial and Systems Engineering Department, King Fahd University of Petroleum and Minerals, Dhahran 31261, Saudi Arabia
[4]Control and Energy Management Laboratory (CEMLab), University of Sfax, Sfax 3038, Tunisia

Corresponding author: Abdul-Wahid A. Saif (awsaif@kfupm.edu.sa)

This work was supported by the King Fahd University of Petroleum and Minerals (KFUPM).

ABSTRACT In this paper, a leader-follower-based cooperative and formation flight control is designed for a group of quadrotors using new forms of fractional sliding mode control (FSMC) strategy accompanied by the potential field algorithm. The FSMC strategy is employed as an inner controller to stabilize each individual UAV quadrotor while the potential field function is used as a formation algorithm (output controller) in order to keep a desired shape formation during the navigation of the fleet. Firstly, the stability of a single quadrotor subjected to external disturbances is addressed by designing an FSMC in addition to a classical PID controller. The FSMC is responsible for stabilizing the altitude and attitude of the vehicle while the responsibility of the PID is to control the two-dimensional (x-y) position of the UAV. Lyapunov-based sliding condition is used in the design of the fractional control strategy to guarantee system stability. The controller's parameters are tuned using the genetic algorithm (GA) to obtain better performance and more robustness against external disturbances. The potential field algorithm is used to generate the paths that are required for the fleet of vehicles to navigate while keeping a prescribed formation shape. This is done by using the attractive potential field to attract the followers toward the leader and the repulsive potential field to repulse every two neighboring followers in order to keep a required distance between them. Simulation results have proved the efficiency of the proposed control system for both the single and multi-agent cases.

INDEX TERMS Sliding mode control, fractional sliding mode control, unmanned aerial vehicle, formation control.

I. INTRODUCTION

In recent years, the study of unmanned aerial vehicles (UAVs) has attracted extensive attention because of their various applications in several fields. UAVs are very useful for both the military and civilian fields. In the field of military, they can be used in several tasks such as carrying radars, cameras, weapons, and other payloads in addition to observing and exploring hostile environments. In the field of civilians, UAVs are used for conducting scientific research, search and rescue tasks, watching natural resources, and different security tasks [1]. Deferent control algorithms have been used to control these vehicles including classical PID [2], implicit PID controller [3], LQR [4], feedback linearization [5], Adaptive feedback linearization [6], back-stepping control [7], sliding mode control [8], adaptive fuzzy control [9], neural network based MPC [10] and several other control algorithms, see the survey in [11].

Multi-UAV formation flight combines both the study of unmanned aerial vehicles with coordination, so it gained

The associate editor coordinating the review of this manuscript and approving it for publication was Guillermo Valencia-Palomo.

the interest of both unmanned systems and control fields. In the cooperative formation flight, a group of UAV vehicles tracks a prescribed path while achieving useful tasks and keeping a required formation shape [12]. Formation flight of UAVs can be achieved using different methodologies such as the leader-follower, virtual structure, and behavioral methodologies. The idea of formation control based on artificial potential field technique was clarified in [13]. The vehicles in this approach travel while they are affected by a field of forces similar to the electric field of the positive and negative charges. The attractive charge represents the required target while the repulsive charges represent obstacles [14]. The authors in [41], [42], [43], [44] discussed fault-tolerant of a set of fixed wing UAV, where synchronization/coordination tracking control scheme with fractional-order calculus are used against actuator and sensor faults. The authors assumed that each UAV will track a given attitude reference attitude. No formation technique is use. The authors in [45] proposed a nonlinear observer-based approach to address the robust cooperative tracking problem and application for heterogeneous spacecraft systems.

Fractional order calculus is the mathematics field that uses an arbitrary order operation when dealing with differentiation and integration. This means that the order can be integer, real, or even complex number [15]. Because of the lack of the methods that solve fractional differential equations, the use of fractional calculus was almost absent. Nowadays, a lot of methods can solve the fractional differential equations and fractional calculus can be applied in different fields of applications. As an effective method to develop the performance of control systems, fractional calculus has been used in different traditional control structures including fractional order Proportional integral derivative (PID) control [16], fractional order optimal control [17], fractional order adaptive control [18] and fractional order sliding mode control [19]. It has been confirmed with evidences that fractional order control systems can outperform integer order control systems [20]. The control of UAV quadrotors using the FSMC has been addressed with using different fractional structures to design the control action. In [21], a FSMC is designed by using an integer order sliding manifold with a fractional order control action. In [22], a fractional manifold with a proportional–fractional order derivative structure was used to design the fractional controller. In [23], without any proportional term, the authors used a combination of an integer order derivative, fractional order derivative and fractional order integral of the state's error to design the sliding surface. In [24], the sliding surface is designed using a combination of integer and fractional order derivatives of the error. In [25] and [26] the fractional order sliding mode controller is designed with using a fractional order manifold that contains fractional order derivative and integral of the error. In [27] an integer order sliding surface with fractional order switching law were used to design the fractional order sliding mode controller. In [28], the authors investigated the reinforcement learning-based control strategy for second-order continuous-time multi-agent systems (MASs) subjected to actuator cyberattacks during affine formation maneuvers.

Fractional order control, also applied to control different physical systems. For example [29], proposed a variable structure control with neural network and optimized fractional-order selection policy for the sensorless telerobotic.

As a powerful technique, the genetic algorithm is used for the tuning of the parameters of several controllers and has been used significantly to tune the parameters of fractional order controllers specially the PID [30], [31] and sliding mode [32], [33] controllers.

The cooperative and formation control for a group of quadrotors UAVs using the fractional control strategies is still limited and not totally studied in the literature of multi-agent systems and cooperative control. This problem will be addressed in this study by proposing a novel fractional sliding mode control (FSMC) strategy to stabilize and achieve the tracking tasks of the attitude and altitude dynamics of UAV quadrotor. This is conducted by selecting a fractional sliding surface, consisting of proportional, integer derivative and fractional derivative of the errors, which results in fractional control input signals. These signals control the altitude and attitude dynamics while a classical PD controller is used to calculate the desired roll (ϕ) and pitch (θ) angles that are required to stabilize the position dynamics in the x and y directions. The famous powerful genetic algorithm (GA) is used to tune the fractional order along with the other parameters of the controller to obtain better system performance. The formation flight control is then studied with using the proposed FSMC as an inner controller to stabilize the individual UAV quadrotors while using the potential field as a formation algorithm (output controller) in order to keep a desired shape formation during the fleet navigation. The Matlab/Simulink environment is used to simulate all the results in this study and the fractional-order modeling and control (FOMCON) toolbox developed by Tepljakov [34] is used for the numerical calculations of the fractional terms.

The paper is organized as follows. Section II gives some preliminary results on the fractional calculus, the dynamic model of the Quadrotor and the Genetic algorithm used for optimization. Section III presents the derivation of the fractional order sliding mode control applied to the model of the Quadrotor. The results of the derive control strategy is tested with simulation and reported in Subsection III-B. The Cooperative and formation control of a set of Quadrotors is given in Section IV and its subsections. Subsection IV-C presents extensive simulation to prove the validity of the control results reported in this section where the Genetic algorithm is used to find optimal values for the controller parameters. Section V conclude this work.

II. PRELIMINARIES

Fractional calculus deals with differentiation and integration of non-integer order differential equation denoted by the fundamental operator ${}_aD_t^{\alpha}$, where a and t represent the bounds

of the operation while α is the fractional order which can be a complex number. It is defined as [26];

$$ {}_aD_t^{\alpha} = \begin{cases} \dfrac{d^{\alpha}}{dt^{\alpha}} & : R(\alpha) > 0, \\ 1 & : R(\alpha) = 0, \\ \displaystyle\int_a^t (d\tau)^{\alpha} & : R(\alpha) < 0 \end{cases} \tag{1} $$

There are three most frequently used definitions for the fractional differentiation-integrals [35]:

i. Grunwald-Letnikov (GL), given by

$$ {}_aD_t^{\alpha} f(t) = \lim_{h \to 0} h^{-\alpha} \sum_{j=0}^{\left[\frac{t-a}{h}\right]} (-1)^j \binom{\alpha}{j} f(t - jh) \tag{2} $$

where the upper limit [.] represents the integer part.

ii. Riemann-Liouville (RL) given by

$$ {}_aD_t^{\alpha} f(t) = \frac{1}{\Gamma(n-\alpha)} \frac{d^n}{dt^n} \int_a^t \frac{f(\tau)}{(t-\tau)^{\alpha-n+1}} d\tau, \quad for\ (n-1 < \alpha < n) \tag{3} $$

where Γ (.) denotes the Euler's gamma function.

iii. Caputo's given by

$$ {}_aD_t^{\alpha} f(t) = \frac{1}{\Gamma(n-\alpha)} \int_a^t \frac{f^n(\tau)}{(t-\tau)^{\alpha-n+1}} d\tau, \quad for\ (n-1 < \alpha < n) \tag{4} $$

Laplace transform technique is useful in solving fractional order differential equations. The Laplace transform of the operator for the above listed function under zero initial conditions is given by;

$$ \mathcal{L}\left\{ {}_0D_t^{\alpha} f(t); s \right\} = s^{\alpha} F(s). \tag{5} $$

However, numerical methods do exist for calculating fractional-order derivatives which are the GL method, continuous and discrete-time approximation techniques and Podlubny's matrix approach. Fortunately, some MATLAB tools come in handy when dealing with such methods [35].

A. DYNAMIC MODEL OF THE QUADROTOR

To identify the UAV quadrotor dynamic model, an inertial and a body fixed reference frames are needed to be considered. The inertial reference frame I, is described by axes X, Y and Z while the body frame B, attached to the vehicle center of mass, is described by axes x_B, y_B, and z_B as shown in Figure 1.

Considering the quadrotor as a rigid body, and based on the Newton-Euler approach, the dynamic model which describes the motion of the vehicle can be obtained as [37]:

$$ \ddot{x} = \frac{\cos(\phi)\sin(\theta)\cos(\varphi) + \sin(\phi)\sin(\varphi)}{m} u_1 + \nu_x \tag{6} $$

$$ \ddot{y} = \frac{\cos(\phi)\sin(\theta)\sin(\varphi) - \sin(\phi)\cos(\varphi)}{m} u_1 + \nu_y \tag{7} $$

$$ \ddot{z} = -g + \frac{\cos(\phi)\cos(\theta)}{m} u_1 + \nu_z \tag{8} $$

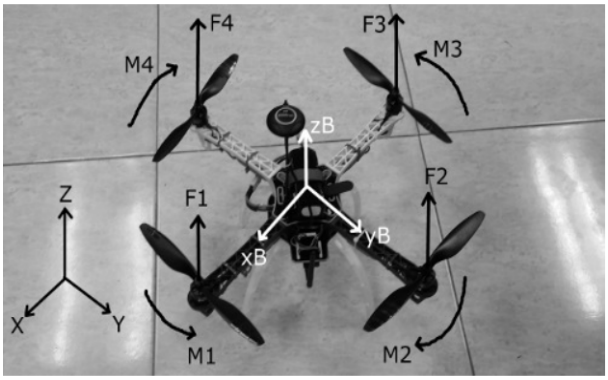

FIGURE 1. The quadrotor with its coordinate systems [36].

$$ \ddot{\phi} = \frac{\dot{\theta}\dot{\varphi}(I_{yy} - I_{zz})}{I_{xx}} + \frac{u_2}{I_{xx}} + \nu_{\phi} \tag{9} $$

$$ \ddot{\theta} = \frac{\dot{\phi}\dot{\varphi}(I_{zz} - I_{xx})}{I_{yy}} + \frac{u_3}{I_{yy}} + \nu_{\theta} \tag{10} $$

$$ \ddot{\varphi} = \frac{\dot{\phi}\dot{\theta}(I_{xx} - I_{yy})}{I_{zz}} + \frac{u_4}{I_{zz}} + \nu_{\varphi} \tag{11} $$

where the terms $\nu_x, \nu_y, \nu_z, \nu_{\phi}, \nu_{\theta}$ and ν_{φ} are unknown bounded perturbation terms.

The quadrotor has four rotors and each rotor is equipped with a motor rotates with an angular velocity ω_i, i = 1, 2 . . . 4. Each motor generates a vertical force F_i and moment M_i which are related to the angular velocities as [38]

$$ F_i = k_F \omega_i^2 $$
$$ M_i = k_M \omega_i^2 $$

where k_F and k_M are the thrust and drag coefficients. The angular velocities are related to the control signals as [38]

$$ \begin{bmatrix} u_1 \\ u_2 \\ u_3 \\ u_4 \end{bmatrix} = \begin{bmatrix} k_F & k_F & k_F & k_F \\ 0 & \ell k_F & 0 & -\ell k_F \\ -\ell k_F & 0 & \ell k_F & 0 \\ k_M & -k_M & k_M & -k_M \end{bmatrix} \begin{bmatrix} \omega_1^2 \\ \omega_2^2 \\ \omega_3^2 \\ \omega_4^2 \end{bmatrix} $$

where ℓ is the length of the quadrotor arm.

B. GENETIC ALGORITHM (GA)

Genetic algorithm (GA) is one of the most useful and powerful Heuristic techniques that are used to minimize a cost (fitness) function based on adjusting some or all the parameters of that cost function. The power of GA comes from the fact that it needs only fitness function evolutions instead of derivatives or other auxiliary knowledge to perform its search. It uses probabilistic evolution rules rather than deterministic rules and deal with a population of candidate solutions to the concrete problem. These solutions are called individuals or chromosomes and evolve iteratively. In a process called selection, the population chromosomes are evaluated using the fitness function in order to select the chromosomes that will be used to generate the new ones for the next generation. Then

the genetic operators, such as crossover and mutation, are used to generate the new individuals. The genetic algorithm can be conducted by using the following steps [39]:

- Step 1. Set the GA parameters such as number of generations, crossover rate, and mutation rate then initialize with a population of random solutions.
- Step 2. Evaluate the fitness function.
- Step 3. Apply crossover and mutation operation to obtain the new generation.
- Step 4. Repeat Steps 2 and 3 until the best value is achieved.

The crossover operator is a technique for sharing features between chromosomes. It combines the characteristics of two parent chromosomes to generate two children, with the possibility that good chromosomes may produce better ones. The mutation operator randomly alters one or more genes of a nominated chromosome such that the organizational variability of the generation increases. In this work the GA is employed to adjust the fractional orders in addition to the control parameters to minimize the tracking errors of the quadrotor system. Therefore, each chromosome of the GA is represented by a vector containing candidate values of the control parameters and the fractional orders (the genes) while the tracking error is used as a cost function that is needed to be minimized.

The total Integral Absolute Error (IAE) is set to be the cost function that is required to be minimized.

$$\mathrm{IAE} = \int_0^\infty \left(|\mathrm{e_x}\,(\mathrm{t})| + \left|\mathrm{e_y}\,(\mathrm{t})\right| + |\mathrm{e_z}\,(\mathrm{t})|\right) \tag{12}$$

where e_x, e_y and e_z are the tracking errors in x, y and z directions respectively. The Matlab function (ga) is used for implementing the genetic algorithm during the control simulations with real coded chromosomes. The population size is set to be 50 for number of genes less than or equal 5 and 200 otherwise. The crossover and mutation probability rates are set to be 0.8 and 0.01 respectively. In every iteration, the GA is set to run the Simulink file of the corresponding system then calculate the total IAE in the step of evaluating the fitness function.

The GA is used to adjust the fractional orders and control parameters of the FSMC control system.

III. FRACTIONAL SLIDING MODE CONTROL (FSMC)

In this section, the quadrotor dynamics is assumed to be affected by external perturbations and a fractional sliding mode control (FSMC) structure is proposed to stabilize its attitude, represented by the Euler angels, in addition to the dynamics in z direction. As shown in Figure 3, FSMC and PD control strategies are designed to stabilize the quadrotor. The FSMC controller is responsible for stabilizing the quadrotor attitude and the dynamics of z position, while the PD controller is working as an outer loop controller to calculate the required roll (ϕ) and pitch (θ) angles which stabilize the position dynamics in the x and y directions.

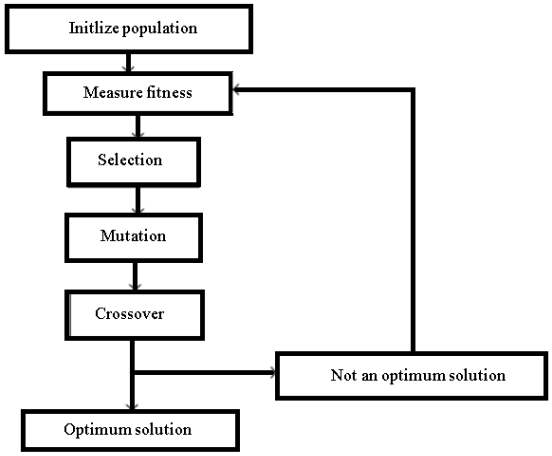

FIGURE 2. GA flow diagram [39].

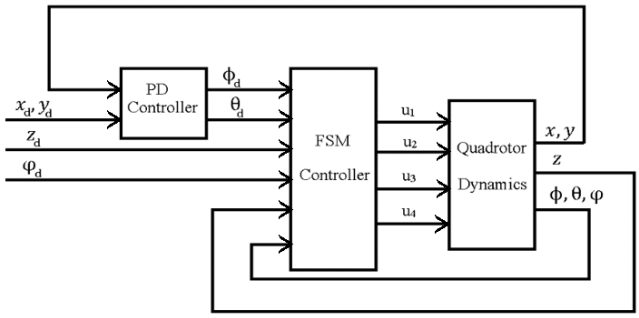

FIGURE 3. Block diagram of the control system.

Assumption: the disturbance signals are unknown but bounded and satisfy:

$$\left\|\nu_{\mathrm{j}}\right\| \leq \kappa_{\mathrm{j}} \quad j = x, y, z, \phi, \theta, \varphi \tag{13}$$

Based on this assumption, the terms ν_x, ν_y, ν_z, ν_ϕ, ν_θ and ν in the dynamics equations (6)-(11) are considered as unknown bounded perturbation terms with real positive bounds κ_x, κ_y, κ_z, κ_ϕ, κ_θ and κ_φ.

A. CONTROL STRATEGY

Equation (8) describes the dynamics of the quadrotor in the z direction. Thus, to control the position in the z direction the tracking error is defined as

$$\mathrm{e_z} = \mathrm{z} - \mathrm{z_d} \tag{14}$$

where z_d is the desired reference signal.

Lemma 1: Let λ_z and ρ_z be real positive parameters. Let

$$\begin{aligned} \dot{\mathrm{e}}_\mathrm{z} &= \dot{\mathrm{z}} - \dot{\mathrm{z}}_\mathrm{d} \\ \ddot{\mathrm{e}}_\mathrm{z} &= \ddot{\mathrm{z}} - \ddot{\mathrm{z}}_\mathrm{d} \end{aligned} \tag{15}$$

Let the fractional order sliding surface be defined as:

$$\mathrm{s_z} = \dot{\mathrm{e}}_\mathrm{z} + \lambda_\mathrm{z} \mathrm{D}^\alpha \mathrm{e_z} + \rho_\mathrm{z} \mathrm{e_z} \tag{16}$$

Then the control law given by

$$\mathrm{u} = \frac{\mathrm{m}}{\cos(\phi)\cos(\theta)} (\mathrm{g} + \ddot{\mathrm{z}}_\mathrm{d} - \lambda_\mathrm{z} \mathrm{D}^\alpha \dot{\mathrm{e}}_\mathrm{z} - \rho_\mathrm{z} \dot{\mathrm{e}}_\mathrm{z})$$

stabilizes the reduced system obtained when

$$\dot{s}_z = \ddot{e}_z + \lambda_z D^{\alpha} \dot{e}_z + \rho_z \dot{e}_z = 0$$

Proof:

The first derivative of s_z is:

$$\dot{s}_z = \ddot{e}_z + \lambda_z D^{\alpha} \dot{e}_z + \rho_z \dot{e}_z = 0 \quad 0 < \alpha < 1 \tag{17}$$

The parameters λ_z and ρ_z should be selected to make e_z in (16) converge exponentially to zero, where,

$$\begin{aligned} \dot{e}_z &= \dot{z} - \dot{z}_d \\ \ddot{e}_z &= \ddot{z} - \ddot{z}_d \end{aligned} \tag{18}$$

Firstly, by considering the disturbance $\nu_z = 0$ in (8), we find the control signal u_{11} which keeps the system on the sliding surface as follows:

From (8) and (18)

$$\ddot{e}_z = -g + \frac{\cos(\phi)\cos(\theta)}{m} u_{11} - \ddot{z}_d \tag{19}$$

where u_{11} is the part of control that is used to keep the system on the sliding surface.

Therefore, $\dot{s}_z$ can be expressed as:

$$\dot{s}_z = -g + \frac{\cos(\phi)\cos(\theta)}{m} u_{11} - \ddot{z}_d + \lambda_z D^{\alpha} \dot{e}_z + \rho_z \dot{e}_z \tag{20}$$

Now u_{11} can be computed such that it makes $\dot{s}_z = 0$, thus:

$$u_{11} = \frac{m}{\cos(\phi)\cos(\theta)} (g + \ddot{z}_d - \lambda_z D^{\alpha} \dot{e}_z - \rho_z \dot{e}_z) \tag{21}$$

The FSMC control strategy proposed in this work includes two control parts u_{11} and u_{12} i.e. $u_1 = u_{11} + u_{12}$. The first part u_{11} is responsible for keeping the system on the sliding surface while the other, u_{12}, makes the system reach the sliding surface. To make the system reach the sliding surface, the additional control signal u_{12} is needed and to be calculated as follows:

The Lyapunov based reachability condition requires [40]

$$s_z \dot{s}_z \leq -\eta_z |s_z| \tag{22}$$

where η_z is a positive constant.

Condition (22) is also used to prove stability of the control system. Therefore, it will be used to design the controller that will guarantee the overall system stability. □

Now, considering the disturbance $\nu_z \neq 0$, $\dot{s}_z$ becomes

$$\begin{aligned} \dot{s}_z = &-g + \frac{\cos(\phi)\cos(\theta)}{m} (u_{11} + u_{12}) \\ &+ \nu_z - \ddot{z}_d + \lambda_z D^{\alpha} \dot{e}_z + \rho_z \dot{e}_z \end{aligned} \tag{23}$$

Substituting u_{11} in (23) and multiplying by s_z

$$s_z \dot{s}_z = s_z \frac{\cos(\phi)\cos(\theta)}{m} u_{12} + s_z \nu_z \tag{24}$$

which will be satisfied with putting:

$$u_{12} = \frac{m}{\cos(\phi)\cos(\theta)} (-k_z \mathrm{sgn}(s_z)) \tag{25}$$

where $k_z = \eta_z + \kappa_z$ and κ_z, as in (13), represents the bound of the perturbation.

TABLE 1. Control parameters.

FOSM Parameters			PD Parameters
$\lambda_z = 7$	$\rho_z = 1$	$k_z = 10$	$K_{px} = 30$
$\lambda_\phi = 1$	$\rho_\phi = 1$	$k_\phi 1.5$	$K_{dx} = 5$
$\lambda_\theta = 1$	$\rho_\theta = 1$	$k_\theta = 1.5$	$K_{py} = 30$
$\lambda_\varphi = 7$	$\rho_\varphi = 1$	$k_\varphi = 10$	$K_{dy} = 5$

Substitute in (24)

$$s_z \dot{s}_z = -(\eta_z + \kappa_z) s_z \mathrm{sgn}(s_z) + s_z \nu_z \tag{26}$$

Since $s_z = |s_z| \mathrm{sgn}(s_z)$

$$s_z \dot{s}_z = -\eta_z |s_z| - \kappa_z |s_z| + s_z \nu_z \tag{27}$$

Now, putting $s_z = |s_z| \mathrm{sgn}(s_z)$ and $\nu_z = |\nu_z| \mathrm{sgn}(\nu_z)$ in the last term leads to

$$s_z \dot{s}_z = -\eta_z |s_z| - |s_z| (\kappa_z + \mathrm{sgn}(s_z)\mathrm{sgn}(\nu_z) |\nu_z|) \tag{28}$$

Now, if s_z and ν_z have the same sign, we have

$$s_z \dot{s}_z = -\eta_z |s_z| - |s_z| (\kappa_z + |\nu_z|) \leq -\eta |s_z| \tag{29}$$

However, if s_z and ν_z have different signs, we obtain

$$s_z \dot{s}_z = -\eta_z |s_z| - |s_z| (\kappa_z - |\nu_z|) \tag{30}$$

From (13), κ_z represents the bound of the perturbation, therefore:

$$|\nu_z| \leq \kappa_z$$

This leads to

$$s_z \dot{s}_z = -\eta_z |s_z| - |s_z| (\kappa_z - |\nu_z|) \leq -\eta |s_z| \tag{31}$$

From (29) and (31), the condition (22) is always satisfied.

Now, u_1 is the summation of the two control signals u_{11} and u_{12} which is given as

$$u_1 = \frac{m}{\cos(\phi)\cos(\theta)} (P_z + g) \tag{32}$$

where

$$P_z = \ddot{z}_d - \lambda_z D^{\alpha} \dot{e}_z - \rho_z \dot{e}_z - k_z \mathrm{sgn}(s_z) \tag{33}$$

For designing the control signals u_2 and u_3, the desired reference signals ϕ_d and θ_d are defined for the angles ϕ and θ respectively. Then, the commonly used small angle approximation is adopted here. Based on this, the dynamics (6), (7), and (9)-(11) take the form:

$$\ddot{x} \approx \tan(\theta) (P_z + g) + \nu_x, \tag{34}$$

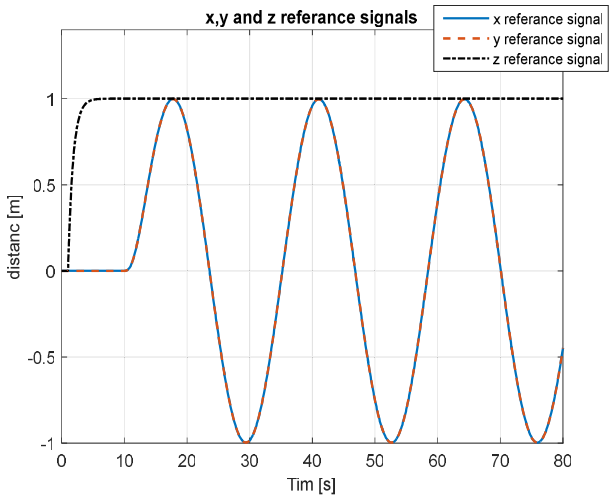

FIGURE 4. The reference signals that are required to be tracked by the system in the x, y and z directions.

TABLE 2. GA tuned control parameters (λ, ρ, α,$\mathbf{K_p}$, $\mathbf{K_d}$).

FOSMC Parameters			PD Parameters
$\lambda_z = 1$	$\rho_z = 0.012$	$\alpha = 0.0124$	$K_{px} = 44.3$
$\lambda_\phi = 1.6$	$\rho_\phi = 0.14$		$K_{dx} = 38.2$
$\lambda_\theta = 3.8$	$\rho_\theta = 0.11$		$K_{py} = 85.9$
$\lambda_\varphi = 7$	$\rho_\varphi = 0.84$		$K_{dy} = 15.5$

$$\ddot{y} \approx -\tan(\phi)\,(P_z{+}g) + \nu_y, \tag{35}$$

$$\ddot{\phi} = \frac{u_2}{I_{xx}} + \nu_\phi, \quad \ddot{\theta} = \frac{u_3}{I_{yy}} + \nu_\theta, \ \ddot{\varphi} = \frac{u_4}{I_{zz}} + \nu_\varphi \tag{36}$$

Now, tan(ϕ) and tan(θ) can be considered as "virtual" input signals in (34) and (35) respectively. Defining the tracking errors e_x and e_y as

$$e_x = x - x_d, \quad e_y = y - y_d, \tag{37}$$

First, assuming ν_x and ν_y are zeros, to find ϕ_d and θ_d that make e_x and e_y converge to zero, a simple PD controller is designed as:

$$\theta_d = \tan^{-1}\left(\frac{1}{P_z{+}g}(\ddot{x}_d - K_{dx}\dot{e}_x - K_{px}e_x)\right) \tag{38}$$

$$\phi_d = -\tan^{-1}\left(\frac{1}{P_z{+}g}\left(\ddot{y}_d - K_{dy}\dot{e}_y - K_{py}e_y\right)\right), \tag{39}$$

For the designed PD control technique to allow the system tracking errors e_x and e_y to approach zero exponentially, the control actions u_2 and u_3 are needed to make θ and ϕ converge to θ_d and ϕ_d as soon as possible. The fractional sliding mode control technique is used again to design the control signals u_2, u_3 and also u_4 with defining the fractional sliding surfaces as:

$$s_j = \dot{e}_j + \lambda_j D^\alpha e_j + \rho_j e_j = 0 \quad j = \phi, \theta, \varphi \tag{40}$$

$$e_j = j - j_d \tag{41}$$

By following the procedure of calculating u_1, the control signals u_2 and u_3 can be obtained as

$$u_2 = I_{xx}(\ddot{\phi}_d - \lambda_\phi D^\alpha \dot{e}_\phi - \rho_\phi \dot{e}_\phi - k_\phi \mathrm{sgn}(s_\phi)) \tag{42}$$

$$u_3 = I_{yy}(\ddot{\theta}_d - \lambda_\theta D^\alpha \dot{e}_\theta - \rho_\theta \dot{e}_\theta - k_\theta \mathrm{sgn}(s_\theta)) \tag{43}$$

and

$$u_4 = I_{zz}(\ddot{\varphi}_d - \lambda_\varphi D^\alpha \dot{e}_\varphi - \rho_\varphi \dot{e}_\varphi - k_\varphi \mathrm{sgn}(s_\varphi)) \tag{44}$$

B. SIMULATION RESULTS

In this section, the MATLAB Simulink environment is used to examine the proposed control strategy. For this purpose, we simulate the results of applying the fractional control strategy on the quadrotor system. The quadrotor system has the following parameters: mass (m) of 1.4 kg and moments of inertia I_{xx}, I_{yy} and I_{zz} of 0.02, 0.02, and 0.04 kg.m^2 respectively. For the controllers we use initially, by trial-and-error, the parameters are shown in Table 1 below, while the fractional order α is shown on the simulation figures since the simulation is run for different values of α.

To examine the performance of the control system, reference signals, and perturbation terms have been given to the system at different times. At time $t = 1s$, a unit step reference is given to be tracked by the quadrotor in the z-direction. Then, at time $t = 10s$, two sine wave signals are given as references in the x and y directions as

$$x_{ref} = y_{ref} = A\sin(wt) \tag{45}$$

where A=1[m], and w= 0.086π [s^{-1}]. The yaw angle is set to equal zero

$$\varphi_{ref} = 0$$

These reference signals are filtered using low pass filters in order to avoid obtaining too high derivative values. Figure 4 shows the used reference signals.

At time $t = 23s$, perturbation terms are introduced as

$$\nu = k_a + k_b \sin(\frac{2\pi t}{T_1}) \tag{46}$$

The perturbations parameters k_a, k_b and T_1 are taken as follows:

$k_a = 0.1$[rad/s^2], $k_b = 0.01$[rad/s^2] and $T_1 = 1.8[s]$.

The perturbation signals are set as:

$$\nu_x = d_y = d_z = 0;$$

$$\nu_\phi = d_\theta = d_\varphi = d$$

During the simulation, saturation terms are used to maintain the input signals within some limits to avoid the high

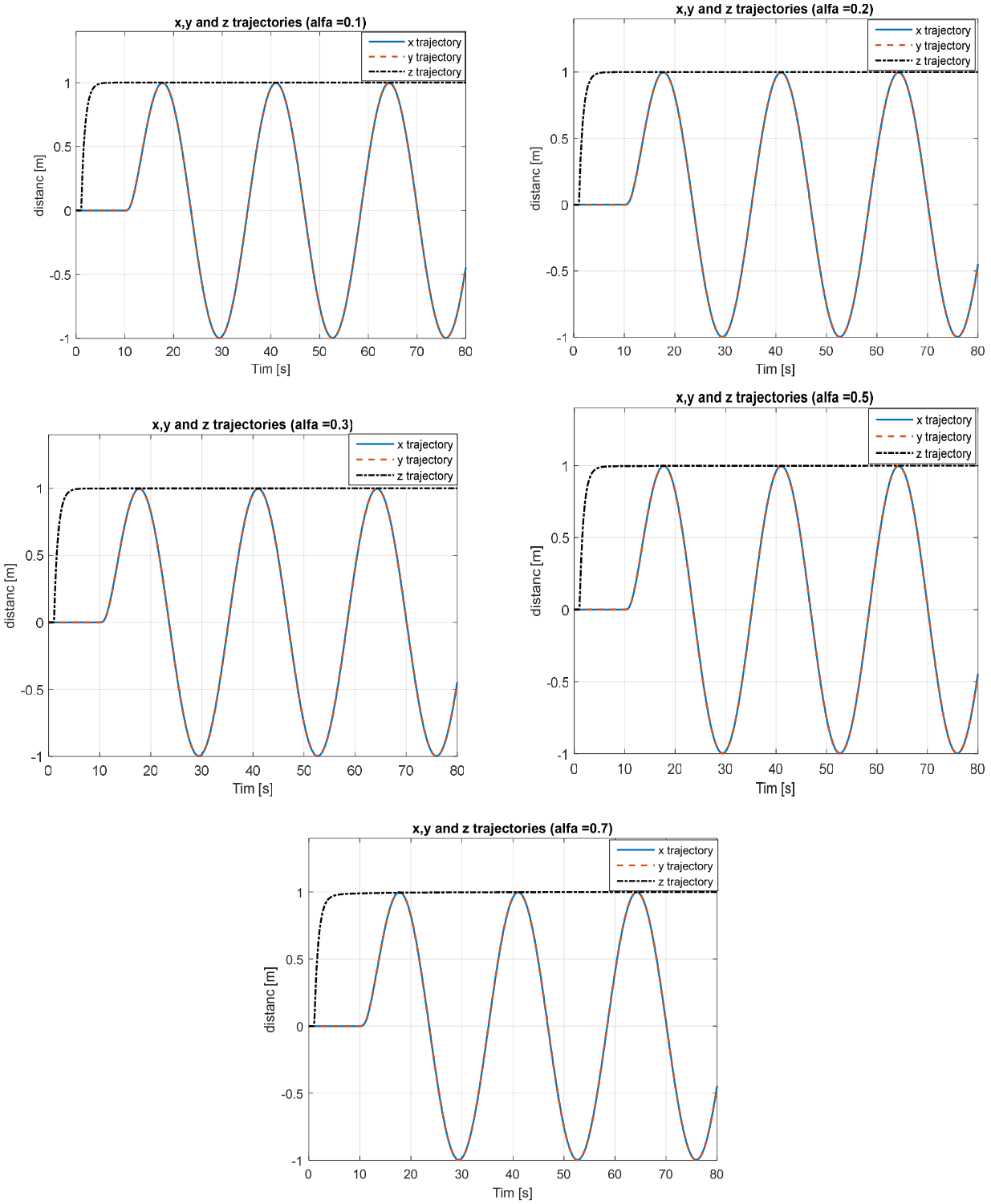

FIGURE 5. The tracking performance and errors of the system with different values of α.

input signals values. These limits are assumed to be [0 30], [−10 10] and [−10 10] for u_1, u_2 and u_3 respectively. The ode45 variable-step solver (the default) is used to solve the required numerical solutions during the simulation of the model associated with the proposed control system and the fractional-order modeling and control (FOMCON) toolbox is used for the numerical calculations of the fractional terms. Moreover, the signum function is implemented as:

$$\text{sgn(s)} = \frac{s}{|s| + \varepsilon}$$

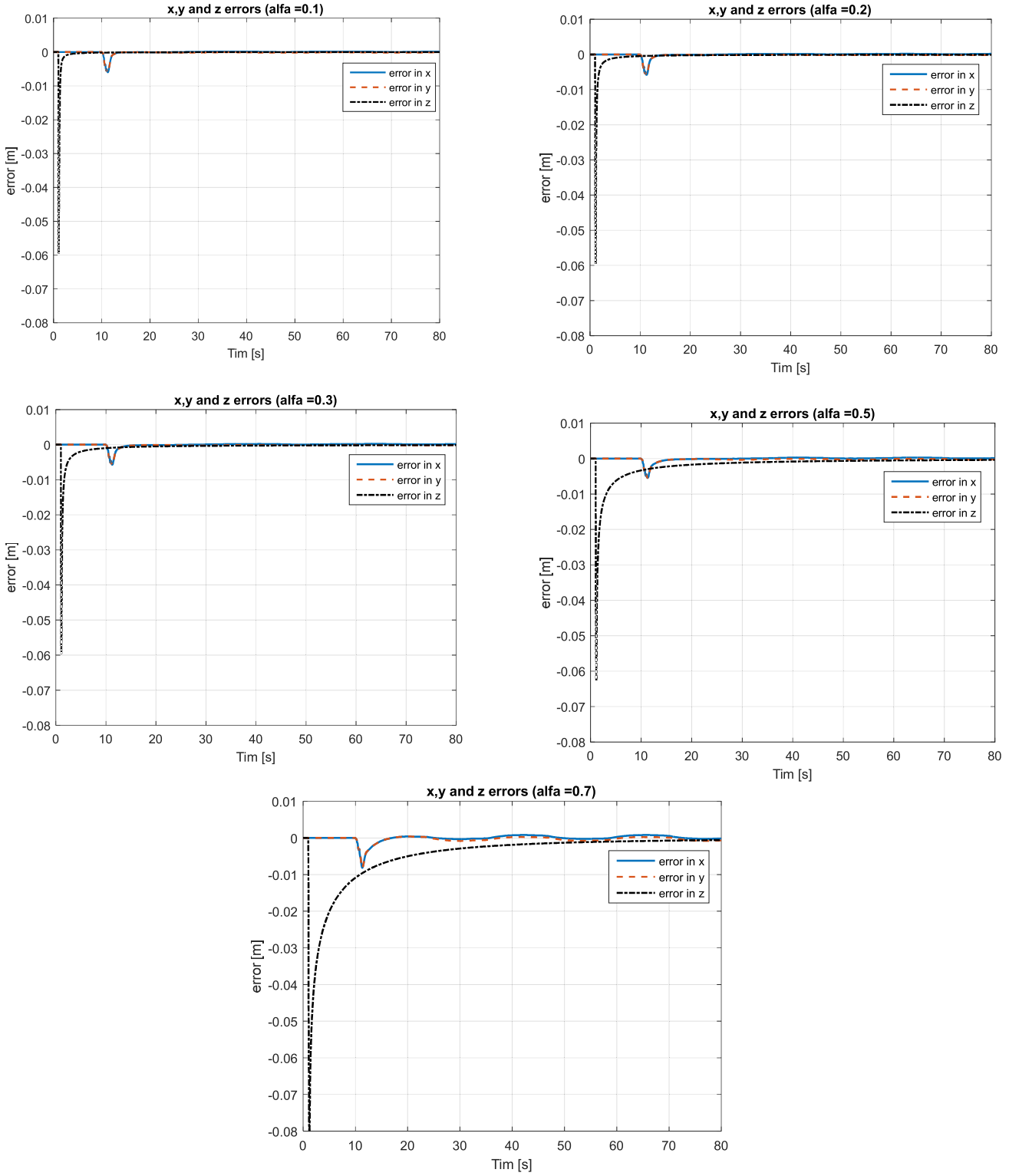

FIGURE 6. The tracking errors of the system with different values of α.

where ε is a small real positive constant and taken here as $\varepsilon = 0.005$.

Figure 5-Figure 7 shows the results of applying the proposed fractional sliding mode control on the system with changing the value of the fractional order α, the values of α are written above each plot. Figure 5 shows the tracking performance while figures 6 and 7 show the tracking errors and control efforts of the system respectively. The

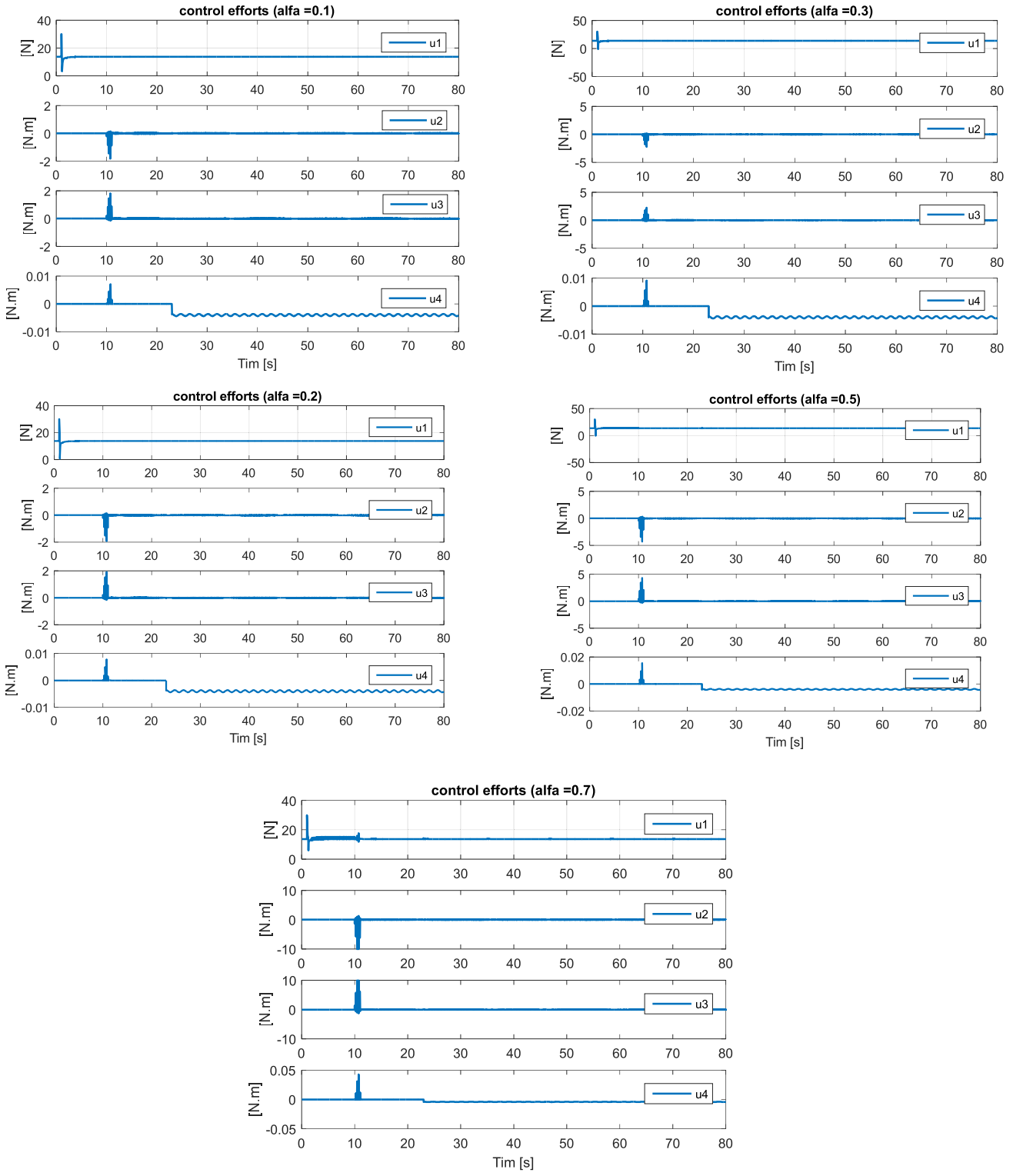

FIGURE 7. The control efforts of the system with different values of α.

figures show deferent behaviors for deferent fractional order α with better performance for the smaller values of α. It is noted that, with increasing the value of the fractional order α, both the raise and settling times increase which leads to slower transient dynamics. Furthermore, the figures show that increasing α leads to lower robustness against the external perturbations and higher input efforts at the time of applying the sin waves references in the x and y

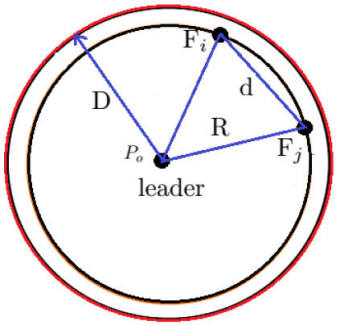

FIGURE 8. The leader with its sensing range D and two followers (Fi and Fj) [41].

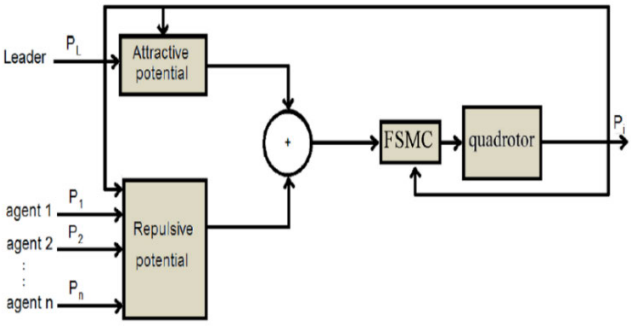

FIGURE 9. The scheme of a follower quadrotor controlled with potential field and FSMC formation control.

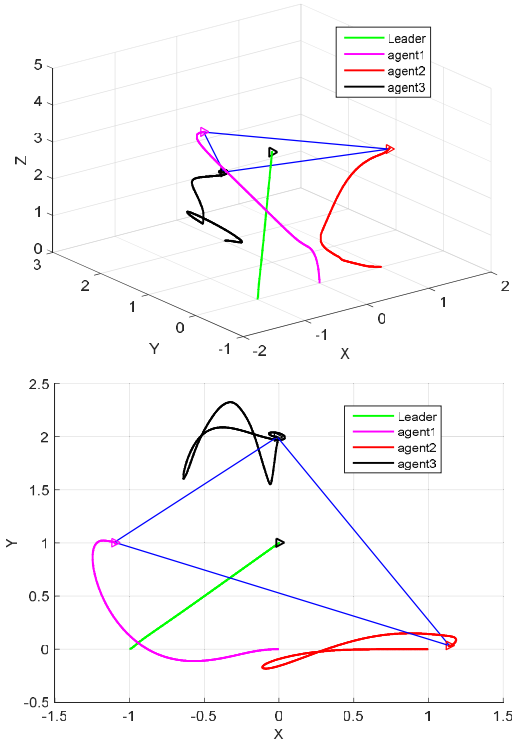

FIGURE 10. Different views of the team performance when the leader moves to the position (1,1,3).

directions. However, it is clear that, the proposed fractional control scheme is able to achieve the required tracking tasks efficiently.

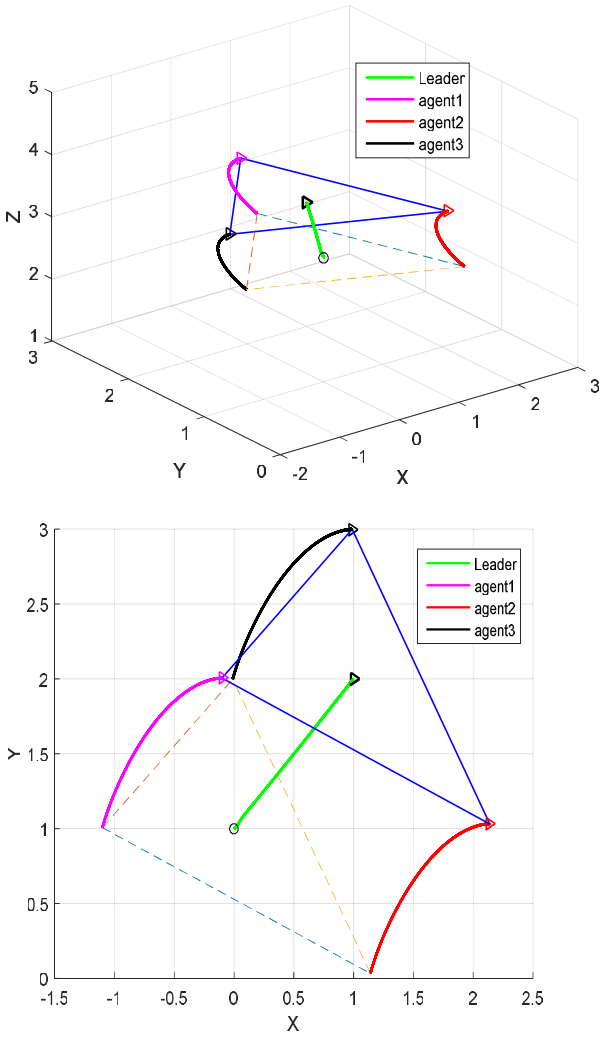

FIGURE 11. Different views of the team performance when the leader moves to the position (2,2,3).

From the Figures it is clear that, the system achieved the best response with $\alpha = 0.1$. However, changing the fractional order α results in different responses of the system. Therefore, in order to achieve better response, the genetic algorithm (GA) will be used in the next section to adjust the system orders α's and parameters.

IV. COOPERATIVE AND FORMATION CONTROL

In this section, cooperative with formation control based on the potential field scheme is studied on a team of quadrotors which designed to navigate with a prescribed flight formation. The vehicles are considered to navigate in a leader-follower formation flight scheme where one of the vehicles is considered as a leader while the others are considered to be followers (agents). The leader navigates with tracking a given reference path while the followers track the leader with keeping a desired formation shape. The potential field technique is used to design the outer controller which generate the paths that guarantee navigation in the required

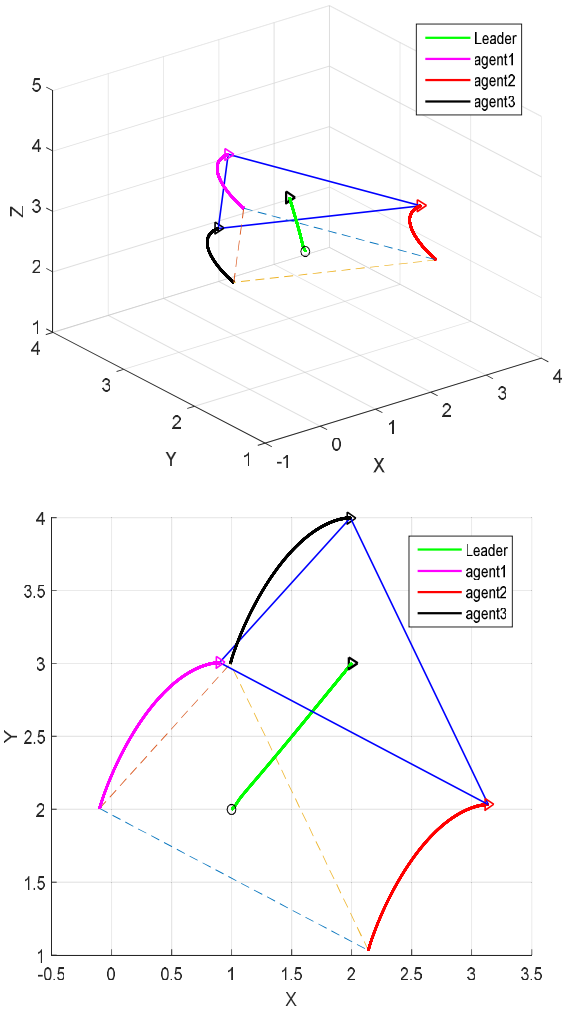

FIGURE 12. Different views of the team performance when the leader moves to the position (3,3,3).

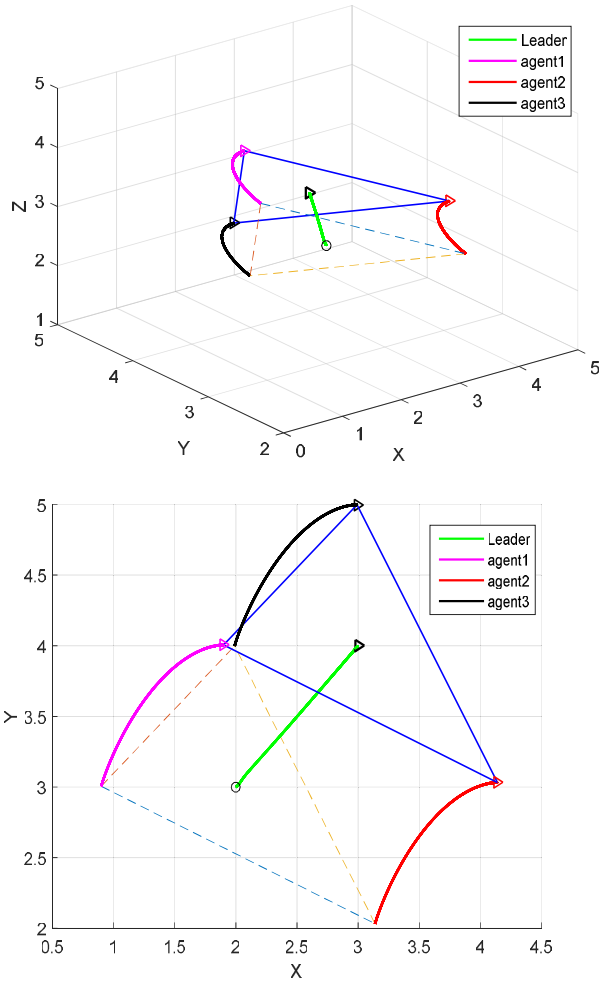

FIGURE 13. Different views of the team performance when the leader moves to the position (4,4,3).

formation polygon. The fractional sliding mode controller (FSMC) is considered as the inner loop controller which is responsible for driving the follower quadrotors to track that produced paths.

A. SHAPE FORMATION

Let each vehicle has a sensing range of D as illustrated in Figure 8. Therefore, each vehicle is able to determine the locations of all its neighbor agents that are positioned inside this sensing range. During their motion, the quadrotors have a task of forming a given polygon with circumcircle of radius R. The leader is required to be positioned at the center while the followers are placed around it. Each two neighboring agents i, j are required to make a distant $\mathrm{d} \leq \mathrm{D}$ from each other. Based on the basics of geometry, R can be defined as:

$$\mathrm{R} = \frac{\mathrm{d}}{2\sin(\pi/\mathrm{n})} \tag{47}$$

where n denotes the number of agents [41].

B. ATTRACTIVE AND REPULSIVE POTENTIAL FIELDS-BASED CONTROL DESIGN

The potential field scheme in [1] and [41] is used to achieve cooperative control for the group of quadrotors. This scheme allows each agent to access the positions of the neighboring agents in addition to the position of the leader. The agents' paths are generated based on the present positions of the leader and the neighboring agents. The application of the attractive and repulsive potential field for formation control will be investigated in this study. The required formation is achieved by using the potential field function to produce the paths that are needed to be followed by the agents. To accomplish this, two potential field functions are needed to be defined, the first one, (U_a), attracts the agents towards the leader, while the second one, (U_r), keeps the distance between each two adjacent agents to be equal or greater than d. The potential field functions U_{att} and U_{rep} are defined as follows:

$$\mathrm{U_a} = \frac{1}{2}\mathrm{k_a}(\mathrm{r_{oi}} - \mathrm{R})^2 \tag{48}$$

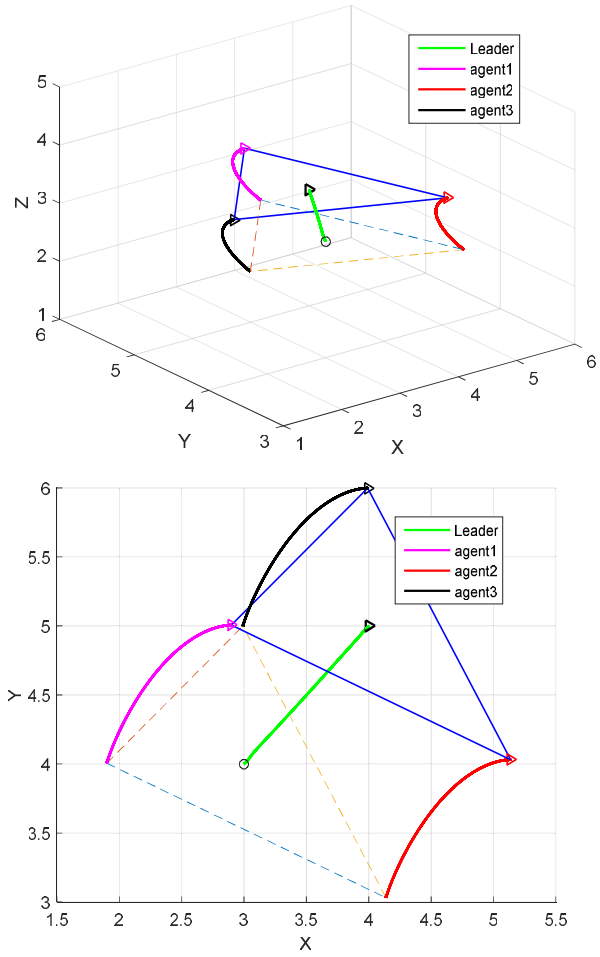

FIGURE 14. Different views of the team performance when the leader moves to the position (5,5,3).

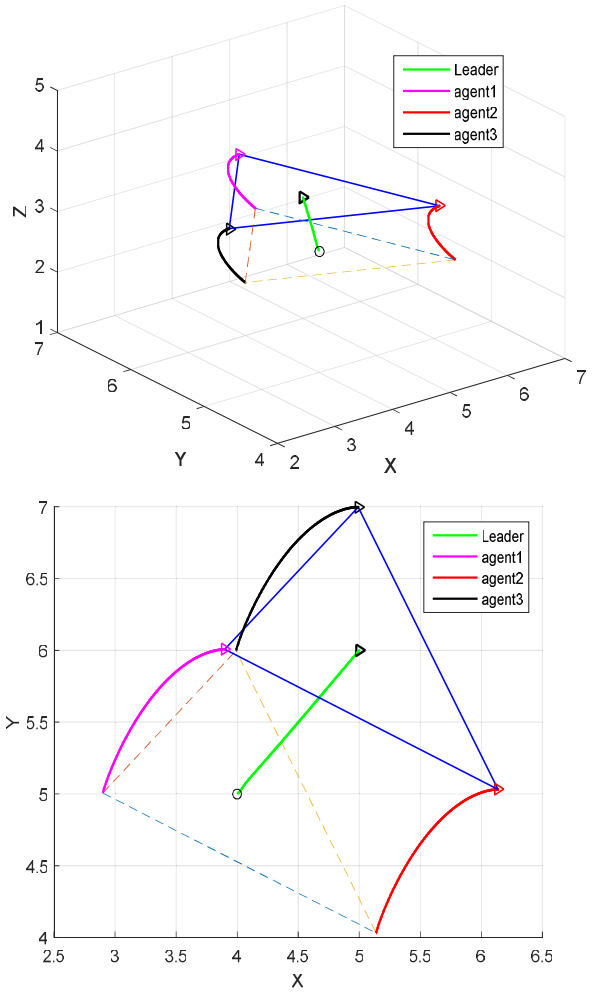

FIGURE 15. Different views of the team performance when the leader moves to the position (6,6,3).

$$U_r = \begin{cases} \frac{1}{2}k_r(r_{i,j}-d)^2 & r_{i,j} < d \\ 0 & \text{otherwise} \end{cases} \quad (49)$$

where:

r_{oi}: The current distance between the i^{th} follower and the leader.

R: The required distance from the leader to the i^{th} agent (the circumcircle radius of the required polygon)

$r_{i,j}$: The current distance between the i^{th} and j^{th} agents.

d: The required distance between the i^{th} and j^{th} agents.

k_a and k_r: are positive design constants

The associated force vector, which represents the negative gradients of the potential fields, is used to control the formation flight of the vehicles group as follows:

$$F = F_o + F_{ij} + Da \quad (50)$$

$$F_o = -\nabla U_a \quad (51)$$

$$F_{i,j} = -\nabla U_r \quad (52)$$

where

F_o : represents the attractive potential (or center potential)

$F_{i,j}$: denotes the repulsive potential

Da: is a damping action

The structure of the cooperative and formation flight control based on the fractional sliding mode control (FSMC) with potential field scheme is shown in Figure 9. The potential field algorithm employs the center potential for attracting the followers towards the leader, which is located at the center of the polygon, and the repulsive potential for repulsing each two adjacent followers to prevent collision. The formation and cooperative flight control algorithm is applied on each follower as a cascaded control structure containing inner and outer loop controllers. The fractional sliding mode controller (FSMC) works as the inner loop control action while the potential field control algorithm represents the outer loop controller.

1) CENTRAL POTENTIAL

From (48) and (51), the attractive potential field of the i^{th} follower is:

$$U_{a_i} = \frac{1}{2}k_a(r_{oi}-R)^2 \quad (53)$$

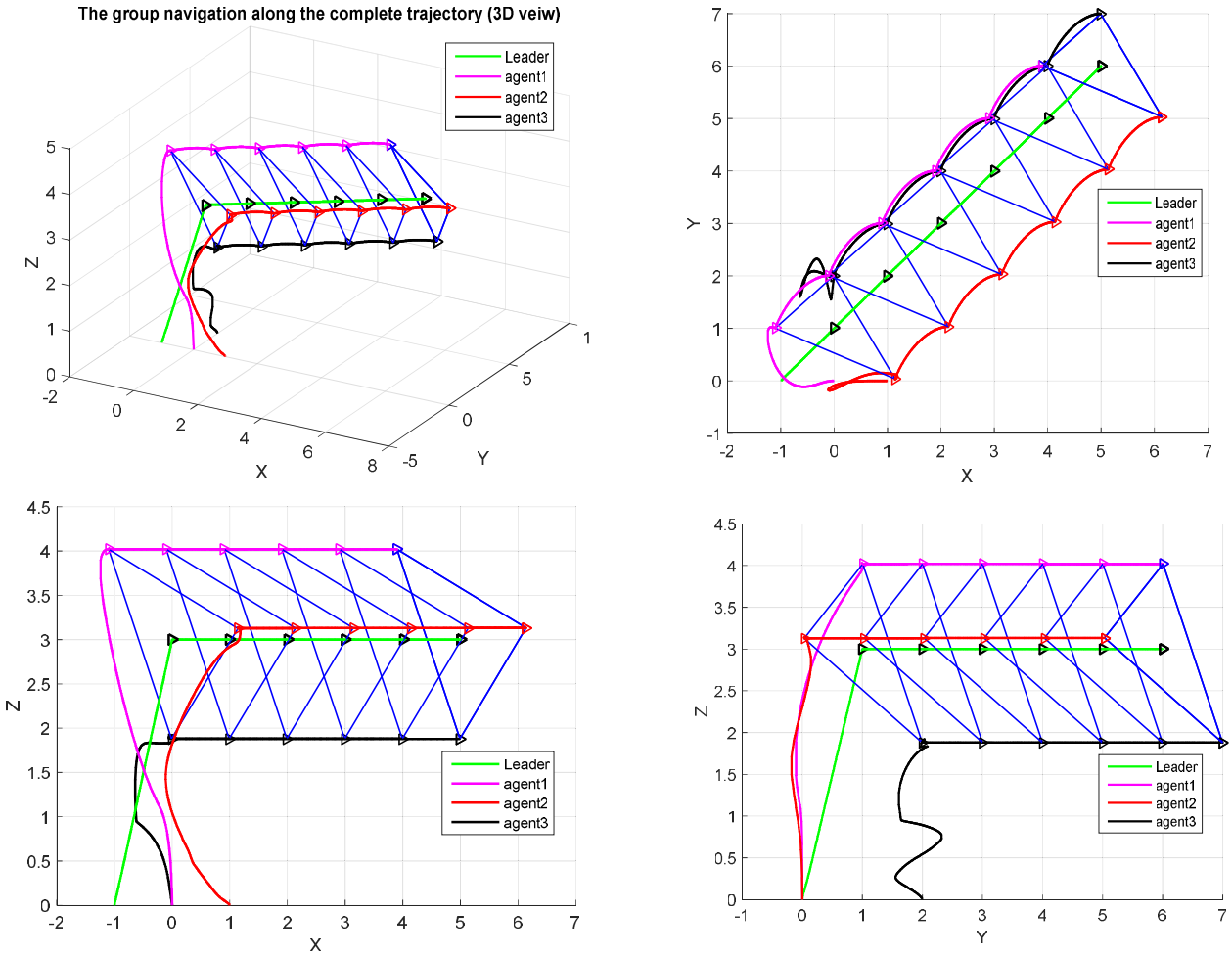

FIGURE 16. The performance of the team along the complete navigation path (different veiws).

$$F_o = -\nabla_{P_i} U_{a_i}(P_i) \tag{54}$$

where $P_i = [x_i, y_i, z_i, \psi_i]^T$ is the current location and heading of the i^{th} agent and r_{oi} can be obtained as:

$$r_{oi} = \sqrt{(x_i - x_o)^2 + (y_i - y_o)^2 + (z_i - z_o)^2 + (\psi_i - \psi_o)^2} \tag{55}$$

The U_{a_i} in equation (53) can be differentiated with respect to P_i to obtain the center potential between the i^{th} follower and the leader as:

$$F_o = -\left(\frac{\partial U_{a_i}}{\partial r_{oi}}\right)\left(\frac{\partial r_{oi}}{\partial P_i}\right) \tag{56}$$

and

$$\frac{\partial U_{a_i}}{\partial r_{oi}} = k_a\,(r_{oi} - R) \tag{57}$$

From (55), let

$$M = (x_i - x_o)^2 + (y_i - y_o)^2 + (z_i - z_o)^2 + (\psi_i - \psi_o)^2 \tag{58}$$

hence:

$$r_{oi} = M^{\frac{1}{2}} \tag{59}$$

The chain rule can be used to differentiate r_{oi} with respect to P_i as:

$$\frac{\partial r_{oi}}{\partial P_i} = \frac{\partial r_{oi}}{\partial M}\frac{\partial M}{\partial P_i} \tag{60}$$

$\frac{\partial r_{oi}}{\partial M}$ can be obtained from(59) as:

$$\frac{\partial r_{oi}}{\partial M} = \frac{1}{2}M^{-\frac{1}{2}} \tag{61}$$

and $\frac{\partial M}{\partial P_i}$ from (58) as:

$$\begin{aligned}\frac{\partial M}{\partial P_i} &= \left[\frac{\partial M}{\partial x_i}\frac{\partial M}{\partial y_i}\frac{\partial M}{\partial z_i}\frac{\partial M}{\partial \psi_i}\right]^T \\ &= \left[2(x_i - x_o)\,2(y_i - y_o)2(z_i - z_o)2(\psi_i - \psi_o)\right]^T \\ &= 2(P_i - P_o)\end{aligned} \tag{62}$$

where $P_o = [x_o, y_o, z_o, \psi_o]^T$ is the current location and heading of the leader. substituting (61) and (62) in (60) to obtain

$$\begin{aligned}\frac{\partial r_{oi}}{\partial P_i} &= M^{-\frac{1}{2}}(P_i - P_o) \\ &= \frac{1}{r_{oi}}(P_i - P_o)\end{aligned} \tag{63}$$

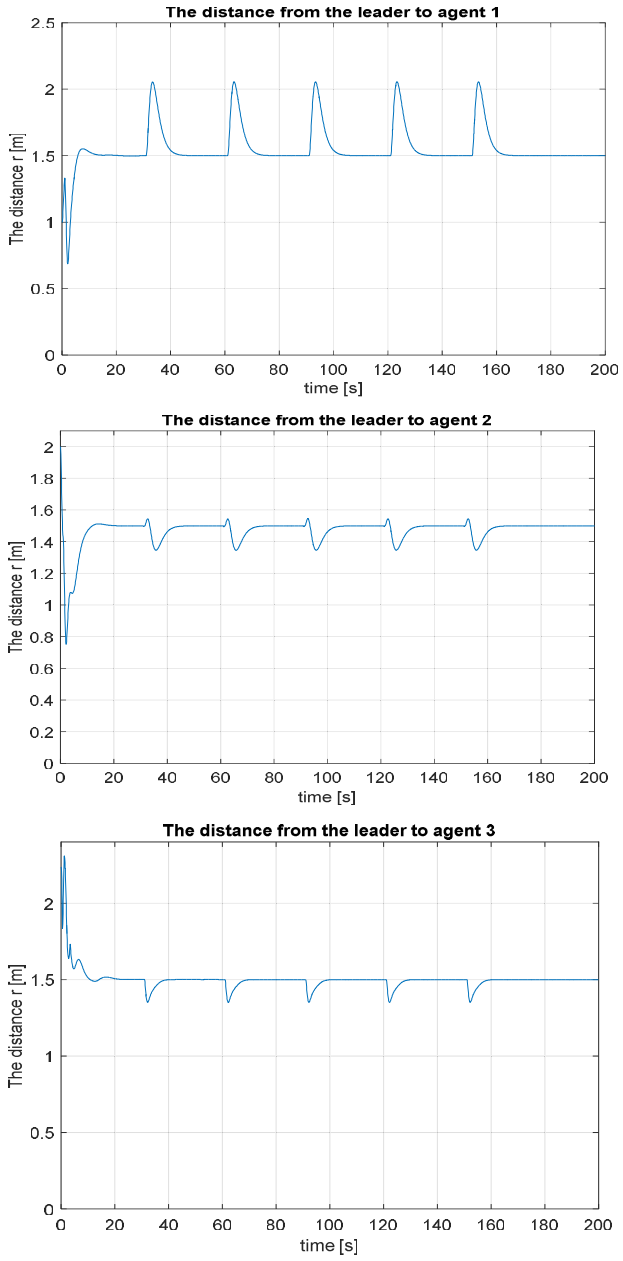

FIGURE 17. The dynamics of the three agents when achieving the distance R from the leader.

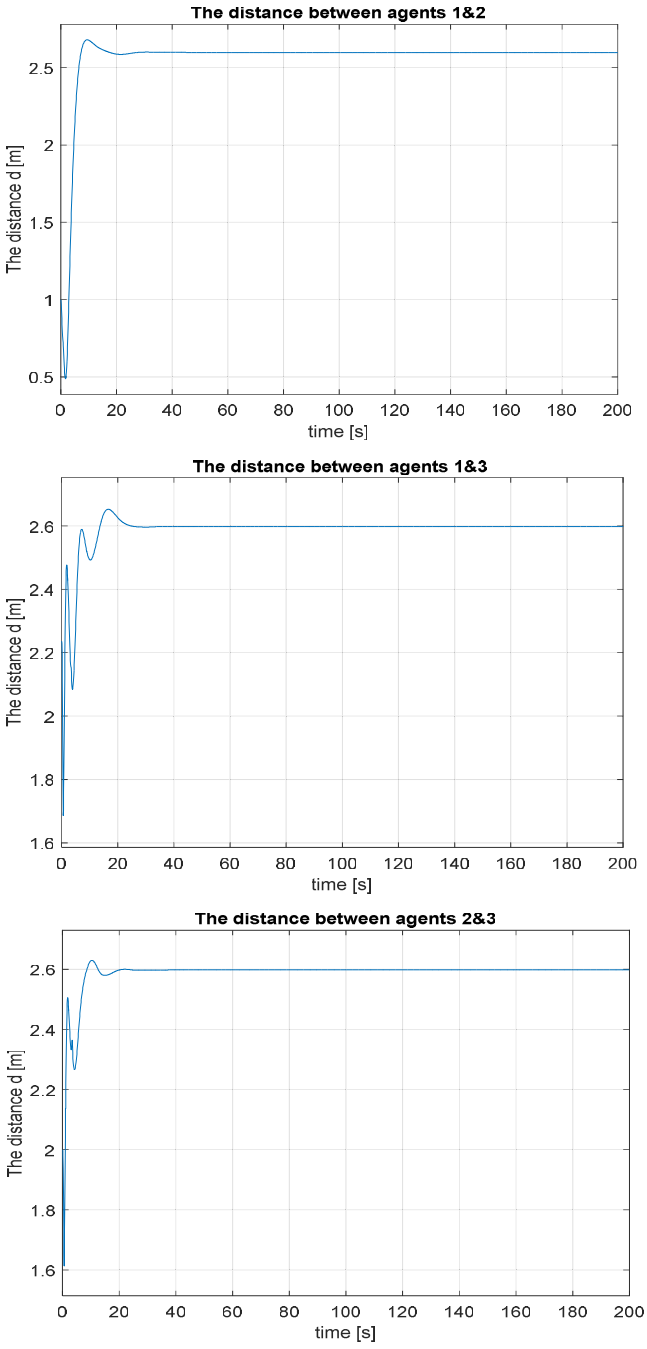

FIGURE 18. The dynamics of each two neighboring agents when keeping the distance d from each other.

Now, by substituting (57) and (63) in (56), the attractive potential can be obtained as:

$$F_o = -k_a \frac{1}{r_{oi}} (r_{oi} - R)(P_i - P_o) \tag{64}$$

2) REPULSIVE POTENTIAL

From (49) and (52), the repulsive potential field of the i^{th} follower is:

$$U_{r_i} = \begin{cases} \frac{1}{2} k_r (r_{i,j} - d)^2 & r_{i,j} < d \\ 0 & \text{otherwise} \end{cases}$$
$$F_{i,j} = -\nabla_{P_i} U_r(P_i, P_j) \tag{65}$$

where $r_{i,j}$ can be obtained as:

$$r_{i,j} = \sqrt{(x_i - x_j)^2 + (y_i - y_j)^2 + (z_i - z_j)^2 + (\psi_i - \psi_j)^2} \tag{66}$$

By following the procedure of calculating F_o, we can obtain the repulsive potential between each two neighboring agents i and j as:

$$F_{i,j} = -k_r \frac{1}{r_{i,j}} (r_{i,j} - d) \left[(P_i - P_j) - (P_j - P_i) \right] \tag{67}$$

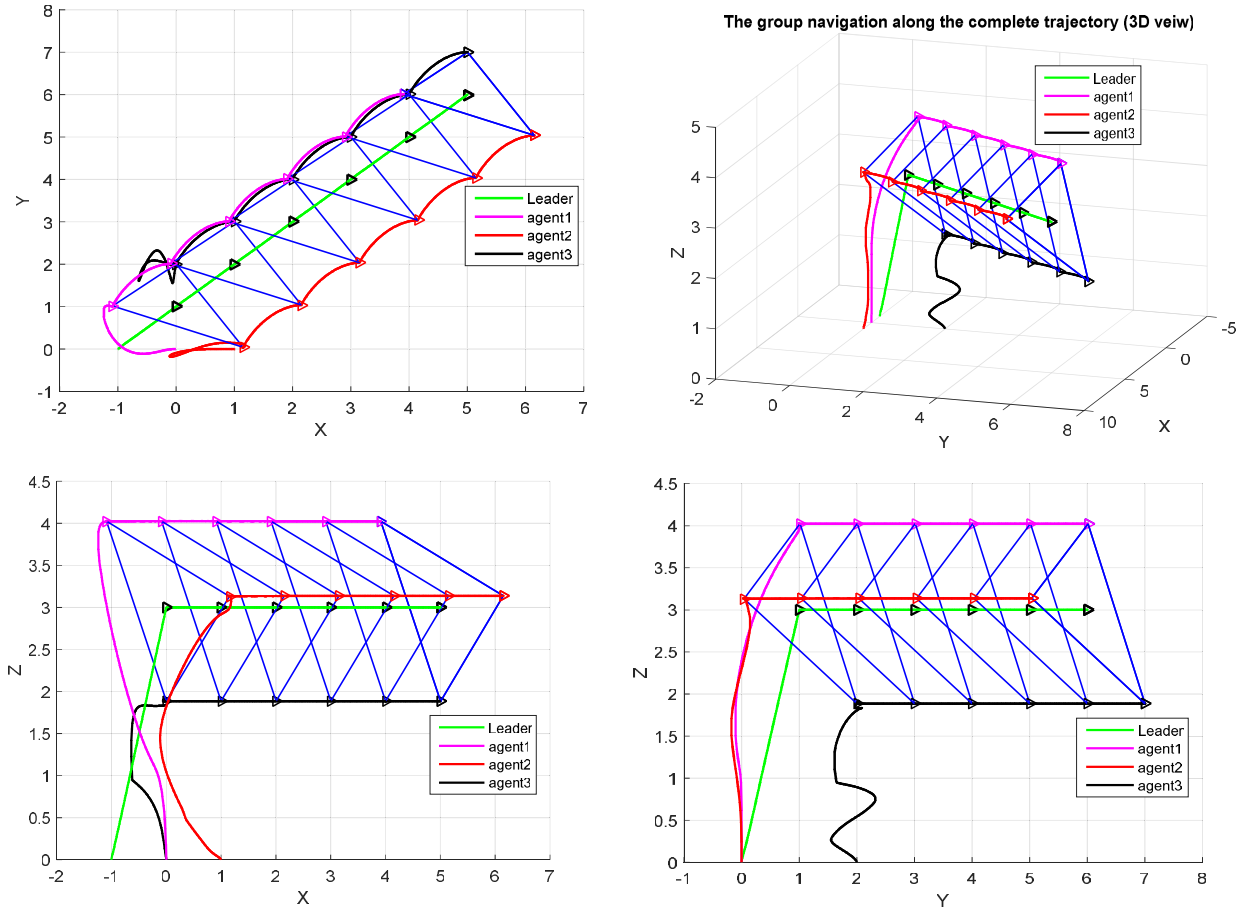

FIGURE 19. The performance of the team along the complete navigation path (diffent veiws).

where, $P_j = [x_j, y_j, z_j, \psi_j]^T$ is the current location and heading of the j^{th} agent.

C. SIMULATION RESULTS

This section shows the results of applying the cooperative and formation control based on the potential field technique with fractional sliding mode (FSMC) control on a team of four quadrotors navigating in space as a leader-followers structure. Each vehicle is controlled by two stages of control, an outer and inner control stages. The cooperative and formation control algorithm is responsible for the outer control stage and this algorithm generates the reference path which is required to be tracked by the follower vehicle. This path is produced based on the present position of the leader and the neighboring followers. The FSMC represents the inner control stage which is responsible for the stability of the quadrotor and tracking tasks. The three followers are set to fly while forming a circle with a radius R around the leader so that the location of the leader represents the circle center. Each follower has to make a distance R from the leader and each two neighboring followers have to make a distance d from each other.

The FSMC is designed with using the genetic algorithm GA to tune the control parameters ρ_z, ρ_ϕ, ρ_θ, ρ_φ, λ_z, λ_ϕ, λ_θ, λ_φ and α in addition to the PD control parameters K_{px}, K_{dx}, K_{py}, and K_{dy} which implies that each chromosome consists of these genes. The remaining parameters are set as $k_z = 2$, $k_\phi = 5$, $k_\theta = 5$, and $k_\varphi = 10$. The cost function (12) is employed for the evaluation process. The search bounds of the control parameters are set to be as following: [1 100] for the PD control parameters, [0.01 0.9] for the fractional order α and [1 10] for the remaining FSMC tuned parameters. The resulting tuned parameters are shown in Table 2. These parameters are used in the simulation process in order to stabilize each follower.

Suppose $R = 1.5m$ and $n = 3$, therefore $d = 2Rsin\left(\frac{\pi}{n}\right) = 2.598$m. The leader has to follow its reference path while the followers use the formation control algorithm for generating their paths which achieve the formation requirements. To prove the efficiency of the proposed control system, the control technique is applied on the quadrotor model and the following simulation results have been achieved. Figures below show the performance of the group, which is controlled by FSMC with potential field formation control, when the leader navigates through different positions along the x-y

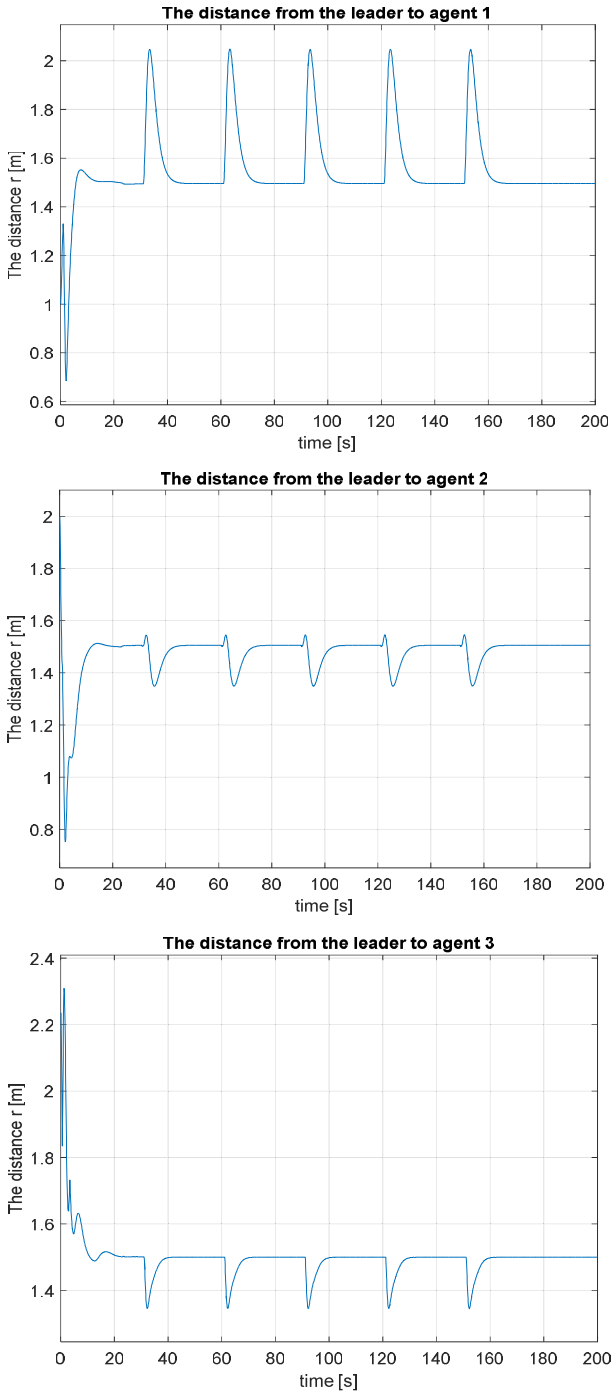

FIGURE 20. The dynamics of the three agents when achieving the distance R from the leader.

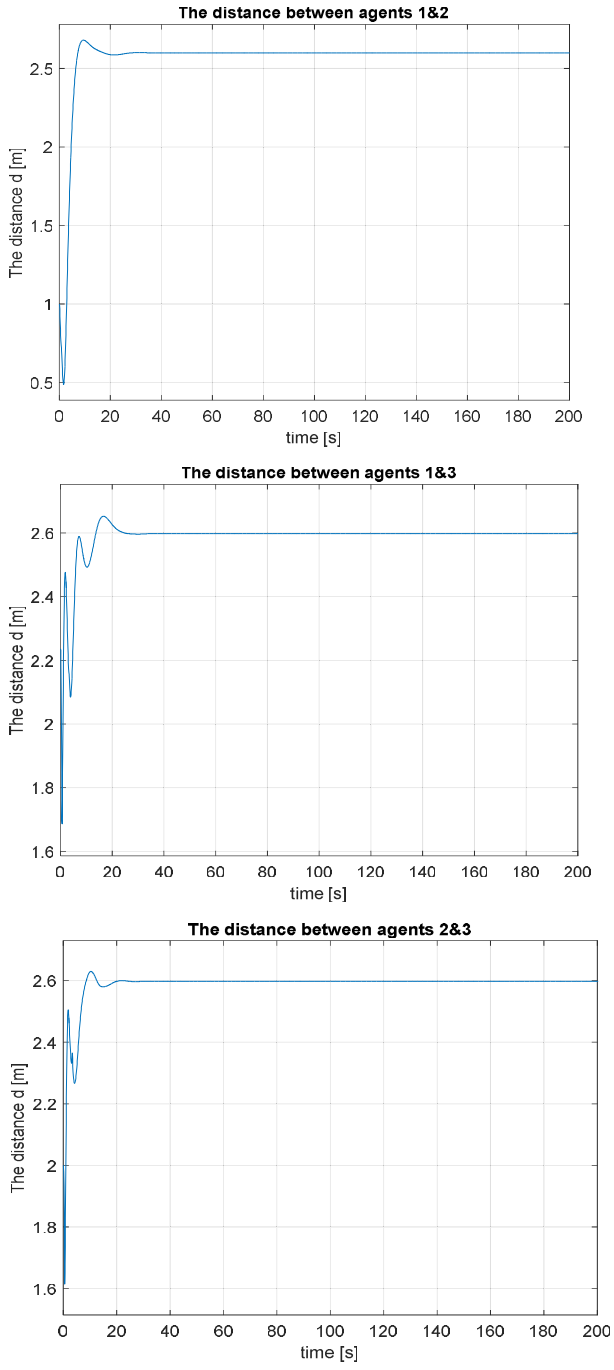

FIGURE 21. The dynamics of each two neighboring agents when keeping the distance d from each other.

direction. The leader is given a reference input in the form of successive steps. While the leader follows its reference, the followers use the potential field algorithm to track it with keeping the required formation. In Figure 10, the leader navigates from the initial position (−1, 0, 0) to the next position which is (1, 1, 3). The first agent navigates from its initial position (0, 0, 0), the second agent from (1, 0, 0), and the third agent from (0, 2, 0) to shape the desired polygon around the leader. In Figure 11-Figure 15, the leader is moving among a sequence of different positions whereas the agents follow the generated paths which form the required formation around it. Figure 16 shows the group of leader and followers quadrotors moving throughout the complete navigation path with keeping the desired formation.

Figure 17 shows the performance of the agents in terms of achieving the required distance of each follower from the leader. This distance is required to be 1.5m and it is clear from

the figures that the formation and FSM controller achieves that efficiently. The agents start the motion from their initial positions then they move to be located at the desired distance. At the beginning of the flight simulation, they take time of around 23s to accomplish this and then, with each movement of the leader, they take around 13s to relocate themselves such that they keep this distance from the leader.

Figure 18 shows the performance of the agents in terms of achieving the required interspatial distance d between each two neighboring followers. This distance d is required to be 2.598m and it is clear from the figures that the formation and FSM controller achieves that efficiently. The agents start the motion from their initial positions then they move to position themselves at the desired interspatial distance. They take time of around 25s to accomplish this and then they navigate through their complete path with keeping this distance from each other.

From these figures, it is clear that the followers are able to track their leader with achieving the desired formation in the 3D plane. All these figures show the efficiency of the proposed FSMC with potential field cooperative and formation control to navigate each vehicle with keeping the desired formation flight.

1) EFFECT OF PERTURBATION

Here, the formation flight based on the fractional sliding mode control (FSMC) with potential field technique is examined when each agent is modeled with considering the effect of bounded perturbation. The perturbation signals are given to the follower's dynamic systems at time t =23s and introduced as:

$$\nu_x = \nu_y = \nu_z = 1 + 0.1\sin(\frac{2\pi t}{1.2})[m/s^2] \quad (68)$$

$$\nu_\varphi = \nu_\theta = \nu_\phi = 1 + 0.3\sin(\frac{2\pi t}{1.8})[rad/s^2] \quad (69)$$

The following figures show the flight formation performance of the group controlled by the FSMC with potential field formation control with the existence of bounded perturbation. Figure 19 shows the group of leader and followers quadrotors moving throughout the complete navigation path with keeping the desired formation.

Figure 20 shows the performance of the group when achieving the required distances between the vehicles. The figures show the efficiency of the proposed FSMC with potential field formation control when navigating each agent with keeping the desired formation flight with the existence of external perturbations. The effect of perturbation is almost eliminated by the FSM controller. However, a very small deviation with fluctuations close to the final goals can be seen in Figure 20.

It is noted from the above figures that, because it is very small, the effect of the perturbation can't be seen in the figures of the team navigation. However, as mentioned before, a very small deviation from the required distance R with fluctuations close to the final goals can be seen in Figure 20.

V. CONCLUSION

In this paper, a cooperative formation flight control is proposed for a team of UAV quadrotors. The control of a single quadrotor with the presence of external perturbations is firstly designed then the control of cooperative flight for multi quadrotors is addressed. The fractional sliding mode control technique is proposed to stabilize the attitude and altitude dynamics of the UAV quadrotor while a classical PD controller is employed as an outer loop controller to calculate the desired roll and pitch angles which stabilize the position dynamics in the x and y directions. The powerful genetic algorithm (GA) is used to adjust the control parameters including the fractional orders to improve the performance of the system based on a desired cost function. Then the cooperative control is addressed based on the FSMC and the potential field approaches. The FSMC is used to stabilize the individual vehicles while the potential field function is used to generate the paths that are required to keep the formation of the fleet. The proposed control system is simulated to examine the validity of the results.

CONFLICT OF INTEREST

The authors declare that they have no conflict of interest.

REFERENCES

[1] A. W. Saif, N. Alabsari, S. E. Ferik, and M. Elshafei, "Formation control of quadrotors via potential field and geometric techniques," *Int. J. Adv. Appl. Sci.*, vol. 7, no. 6, pp. 82–96, Jun. 2020, doi: 10.21833/ijaas.2020.06.011.

[2] J. Li and Y. Li, "Dynamic analysis and PID control for a quadrotor," in *Proc. IEEE Int. Conf. Mechatronics Autom.*, Aug. 2011, pp. 573–578.

[3] S. Wang, A. Polyakov, and G. Zheng, "Quadrotor stabilization under time and space constraints using implicit PID controller," *J. Franklin Inst.*, vol. 359, no. 4, pp. 1505–1530, Mar. 2022, doi: 10.1016/j.jfranklin.2022.01.002.

[4] E. Okyere, A. Bousbaine, G. T. Poyi, A. K. Joseph, and J. M. Andrade, "LQR controller design for quad-rotor helicopters," *J. Eng.*, vol. 2019, no. 17, pp. 4003–4007, Jun. 2019.

[5] M. Alejandro Lotufo, L. Colangelo, and C. Novara, "Feedback linearization for quadrotors UAV," 2019, *arXiv:1906.04263*.

[6] A. Eltayeb, M. F. Rahmat, and M. A. Mohd Basri, "Adaptive feedback linearization controller for stabilization of quadrotor UAV," *Int. J. Integr. Eng.*, vol. 12, no. 4, pp. 1–17, Apr. 2020.

[7] O. García, P. Ordaz, O.-J. Santos-Sánchez, S. Salazar, and R. Lozano, "Backstepping and robust control for a quadrotor in outdoors environments: An experimental approach," *IEEE Access*, vol. 7, pp. 40636–40648, 2019.

[8] H. Rios, R. Falcon, O. A. Gonzalez, and A. Dzul, "Continuous sliding-mode control strategies for quadrotor robust tracking: Real-time application," *IEEE Trans. Ind. Electron.*, vol. 66, no. 2, pp. 1264–1272, Feb. 2019, doi: 10.1109/TIE.2018.2831191.

[9] C. Li, Y. Wang, and X. Yang, "Adaptive fuzzy control of a quadrotor using disturbance observer," *Aerosp. Sci. Technol.*, vol. 128, Sep. 2022, Art. no. 107784, doi: 10.1016/j.ast.2022.107784.

[10] B. Jiang, B. Li, W. Zhou, L.-Y. Lo, C.-K. Chen, and C.-Y. Wen, "Neural network based model predictive control for a quadrotor UAV," *Aerospace*, vol. 9, no. 8, p. 460, 2022.

[11] T. P. Nascimento and M. Saska, "Position and attitude control of multi-rotor aerial vehicles: A survey," *Annu. Rev. Control*, vol. 48, pp. 129–146, Jan. 2019.

[12] L. Di, "Cognitive formation flight in multi-unmanned aerial vehicle-based personal remote sensing systems," Utah State Univ., 2011.

[13] O. Khatib, "Real-time obstacle avoidance for manipulators and mobile robots," *Int. J. Robot. Res.*, vol. 5, no. 1, pp. 90–98, Mar. 1986.

[14] X. Li, D. Zhu, and Y. Qian, "A survey on formation control algorithms for multi-AUV system," *Unmanned Syst.*, vol. 2, no. 4, pp. 351–359, 2014.

[15] R. Matušu, "Application of fractional order calculus to control theory," *Int. J. Math. Model. Methods Appl. Sci.*, vol. 5, no. 7, pp. 1162–1169, 2011.

[16] A. Tepljakov, E. Petlenkov, and J. Belikov, "FOPID controller tuning for fractional FOPDT plants subject to design specifications in the frequency domain," in *Proc. Eur. Control Conf. (ECC)*, Jul. 2015, pp. 3502–3507.

[17] M. H. Heydari, M. R. Hooshmandasl, F. M. Maalek Ghaini, and C. Cattani, "Wavelets method for solving fractional optimal control problems," *Appl. Math. Comput.*, vol. 286, pp. 139–154, Aug. 2016.

[18] Z. M. Odibat, "Adaptive feedback control and synchronization of non-identical chaotic fractional order systems," *Nonlinear Dyn.*, vol. 60, no. 4, pp. 479–487, Jun. 2010.

[19] J. Wang, C. Shao, and Y.-Q. Chen, "Fractional order sliding mode control via disturbance observer for a class of fractional order systems with mismatched disturbance," *Mechatronics*, vol. 53, pp. 8–19, Aug. 2018, doi: 10.1016/j.mechatronics.2018.05.006.

[20] Y. Chen, I. Petras, and D. Xue, "Fractional order control—A tutorial," in *Proc. Amer. Control Conf.*, Jun. 2009, pp. 1397–1411, doi: 10.1109/ACC.2009.5160719.

[21] C. Izaguirre-Espinosa, A. J. Muñoz-Vazquez, A. Sanchez-Orta, V. Parra-Vega, and I. Fantoni, "Fractional-order control for robust position/yaw tracking of quadrotors with experiments," *IEEE Trans. Control Syst. Technol.*, vol. 27, no. 4, pp. 1645–1650, Jul. 2019, doi: 10.1109/TCST.2018.2831175.

[22] H. Farbakhsh, M. Tavakoli-Kakhki, H. D. Taghirad, R. Azarmi, and F. Padula, "Fractional order fast terminal sliding mode controller design with finite-time convergence: Application to quadrotor UAV," in *Proc. 26th IEEE Int. Conf. Emerg. Technol. Factory Autom. (ETFA)*, Sep. 2021, pp. 1–7, doi: 10.1109/etfa45728.2021.9613288.

[23] M. Labbadi and M. Cherkaoui, "Adaptive fractional-order nonsingular fast terminal sliding mode based robust tracking control of quadrotor UAV with Gaussian random disturbances and uncertainties," *IEEE Trans. Aerosp. Electron. Syst.*, vol. 57, no. 4, pp. 2265–2277, Aug. 2021.

[24] M. Labbadi and H. E. Moussaoui, "An improved adaptive fractional-order fast integral terminal sliding mode control for distributed quadrotor," *Math. Comput. Simul.*, vol. 188, pp. 120–134, Oct. 2021, doi: 10.1016/j.matcom.2021.03.039.

[25] M. Labbadi, Y. Boukal, M. Cherkaoui, and M. Djemai, "Fractional-order global sliding mode controller for an uncertain quadrotor UAVs subjected to external disturbances," *J. Franklin Inst.*, vol. 358, no. 9, pp. 4822–4847, Jun. 2021, doi: 10.1016/j.jfranklin.2021.04.032.

[26] M. Pouzesh and S. Mobayen, "Event-triggered fractional-order sliding mode control technique for stabilization of disturbed quadrotor unmanned aerial vehicles," *Aerosp. Sci. Technol.*, vol. 121, Feb. 2022, Art. no. 107337, doi: 10.1016/j.ast.2022.107337.

[27] M. Labbadi, A. J. Muñoz-Vázquez, M. Djemai, Y. Boukal, M. Zerrougui, and M. Cherkaoui, "Fractional-order nonsingular terminal sliding mode controller for a quadrotor with disturbances," *Appl. Math. Model.*, vol. 111, pp. 753–776, Nov. 2022, doi: 10.1016/j.apm.2022.07.016.

[28] S. El-Ferik, M. Maaruf, F. M. Al-Sunni, A. A. Saif, and M. M. A. Dhaifallah, "Reinforcement learning-based control strategy for multi-agent systems subjected to actuator cyberattacks during affine formation maneuvers," *IEEE Access*, vol. 11, pp. 77656–77668, 2023, doi: 10.1109/ACCESS.2023.3296741.

[29] Z. Ma, Z. Liu, P. Huang, and Z. Kuang, "Adaptive fractional-order sliding mode control for admittance-based telerobotic system with optimized order and force estimation," *IEEE Trans. Ind. Electron.*, vol. 69, no. 5, pp. 5165–5174, May 2022.

[30] H. Saribas and S. Kahvecioglu, "PSO and GA tuned conventional and fractional order PID controllers for quadrotor control," *Aircr. Eng. Aerosp. Technol.*, vol. 93, no. 7, pp. 1243–1253, Sep. 2021.

[31] H. L. Maurya, L. Behera, and N. K. Verma, "Trajectory tracking of quad-rotor UAV using fractional order PI^{μ} D^{λ} controller," in *Computational Intelligence: Theories, Applications and Future Directions*. Cham, Switzerland: Springer, 2019, pp. 171–186.

[32] H. Delavari, R. Ghaderi, A. Ranjbar, and S. Momani, "Fuzzy fractional order sliding mode controller for nonlinear systems," *Commun. Nonlinear Sci. Numer. Simul.*, vol. 15, no. 4, pp. 963–978, Apr. 2010.

[33] S. Labdai, L. Chrifi-Alaoui, S. Drid, L. Delahoche, and P. Bussy, "Real-time implementation of an optimized fractional sliding mode controller on the quanser-aero helicopter," in *Proc. Int. Conf. Control, Autom. Diagnosis (ICCAD)*, Oct. 2020, pp. 1–6.

[34] A. Tepljakov, "FOMCON: Fractional-order modeling and control toolbox," in *Fractional-Order Modeling and Control of Dynamic Systems*. Cham, Switzerland: Springer, 2017, pp. 107–129.

[35] I. Petràs, *Fractional Derivatives, Fractional Integrals, and Fractional Differential Equations in Matlab*. Rijeka, Croatia: InTechOpen, 2011.

[36] A. Govea-Vargas, R. Castro-Linares, M. Duarte-Mermoud, N. Aguila-Camacho, and G. Ceballos-Benavides, "Fractional order sliding mode control of a class of second order perturbed nonlinear systems: Application to the trajectory tracking of a quadrotor," *Algorithms*, vol. 11, no. 11, p. 168, Oct. 2018, doi: 10.3390/a11110168.

[37] M. J. Reinoso, L. I. Minchala, P. Ortiz, D. F. Astudillo, and D. Verdugo, "Trajectory tracking of a quadrotor using sliding mode control," *IEEE Latin Amer. Trans.*, vol. 14, no. 5, pp. 2157–2166, May 2016.

[38] D. Mellinger. (2012). *Trajectory Generation and Control For Quadrotors Daniel Mellinger*. [Online]. Available: https://repository.upenn.edu/handle/20.500.14332/32133

[39] A. Jayachitra and R. Vinodha, "Genetic algorithm based PID controller tuning approach for continuous stirred tank reactor," *Adv. Artif. Intell.*, vol. 2014, pp. 1–8, Dec. 2014, doi: 10.1155/2014/791230.

[40] J.-J. E. Slotine and W. Li, *Applied Nonlinear Control*, vol. 199. Upper Saddle River, NJ, USA: Prentice-Hall, 1991.

[41] O. Alburaiki, "Leader–follower SLAM based navigation and fleet management control," M.S. thesis, King Fahd Univ. Petroleum Minerals, KSA, 2012.

[42] Z. Yu, Y. Zhang, B. Jiang, C.-Y. Su, J. Fu, Y. Jin, and T. Chai, "Fractional-order adaptive fault-tolerant synchronization tracking control of networked fixed-wing UAVs against actuator-sensor faults via intelligent learning mechanism," *IEEE Trans. Neural Netw. Learn. Syst.*, vol. 32, no. 12, pp. 5539–5553, Dec. 2021.

[43] Z. Yu et al., "Refined fractional-order fault-tolerant coordinated tracking control of networked fixed-wing UAVs against faults and communication delays via double recurrent perturbation FNNs," *IEEE Trans. Cybern.*, vol. 54, no. 2, pp. 1189–1201, 2022.

[44] Z. Yu, Y. Zhang, B. Jiang, C.-Y. Su, J. Fu, Y. Jin, and T. Chai, "Enhanced recurrent fuzzy neural fault-tolerant synchronization tracking control of multiple unmanned airships via fractional calculus and fixed-time prescribed performance function," *IEEE Trans. Fuzzy Syst.*, vol. 30, no. 10, pp. 4515–4529, Oct. 2022.

[45] B. Wang, W. Chen, B. Zhang, P. Shi, and H. Zhang, "A nonlinear observer-based approach to robust cooperative tracking for heterogeneous spacecraft attitude control and formation applications," *IEEE Trans. Autom. Control*, vol. 68, no. 1, pp. 400–407, Jan. 2023.

NAJIB ALABSARI received the B.Sc. degree from the Mechatronics Engineering Department, Baghdad University, Iraq, and the M.Sc. and Ph.D. degrees from the Control and Instrumentation Engineering Department, King Fahd University of Petroleum and Minerals, Dhahran, Saudi Arabia. His research interests include control of mobile robotics and unmanned aerial vehicles, intelligent control systems, multi-agent and cooperative control, robust control, optimization, and heuristic search algorithms.

ABDUL-WAHID A. SAIF received the B.Sc. degree from the Physics Department, King Fahd University of Petroleum and Minerals (KFUPM), Dhahran, Saudi Arabia, the M.Sc. degree from the Systems Engineering Department, KFUPM, and the Ph.D. degree from the Control and Instrumentation Group, Department of Engineering, Leicester University, Leicester, U.K. After finishing the Ph.D. studies, he joined as a Research Assistant with the Systems Engineering Department and a Lecturer with the Electrical Engineering Department and the Physics Department, KFUPM. He is currently a Professor of control and instrumentation with the Control and Instrumentation Engineering Department (CIE), KFUPM. He taught several courses in modeling and simulation, digital control, digital systems, microprocessors and microcontrollers in automation, optimization, numerical methods, PLCs, process control, and control system design. He has published more than 115 papers, patents, book chapters, and technical reports in reputable journals and conferences. His research interests include simultaneous and strong stabilization, robust control and H8-optimization, instrumentation, and computer control.

SAMI EL-FERIK received the B.Sc. degree in electrical engineering from Laval University, Canada, the M.S. degree in control and automation from the Department of Electrical and Computer Engineering, École Polytechnique, and the Ph.D. degree in control and automation from the University of Montreal, Montreal, Canada. He is currently a Professor with the Control and Instrumentation Engineering Department and the Director of the Interdisciplinary Research Center for Smart Mobility and Logistics, King Fahd University of Petroleum and Minerals (KFUPM). His Ph.D. work was on flexible manufacturing systems modeling and control and was co-supervised by mechanical engineering. His Master's degree on the identification and optimal control of a stochastic electrical load. After completing the Ph.D. studies and postdoctoral positions in analysis and control of discrete event systems, he worked at Pratt and Whitney Canada as a Senior Staff Control Analyst within the Research and Development Center of Systems, Controls, and Accessories. His research interests include sensing, monitoring, and control with strong multidisciplinary research and applications. His research contributions are in control of the autonomous single-domain and multi-domain multi-agent systems, unmanned systems UxV, biological models of a fleet of unmanned aerial vehicles, process control and control loop performance-monitoring, control of systems with delays, modeling, and control of stochastic systems, analysis of network stability, condition monitoring, and condition-based maintenance.

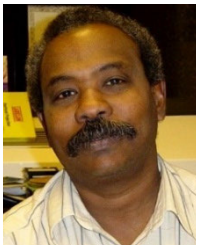

SALIH DUFFUAA received the Ph.D. degree in operations research from The University of Texas at Austin. He is currently a Professor of industrial engineering and operations research with the Industrial and Systems Engineering Department, King Fahd University of Petroleum and Minerals (KFUPM), Dhahran, Saudi Arabia. He has published extensively. His work has appeared in journals, such as *Journal of Optimization Theory and Applications*, *European Journal of Operational Research*, *Engineering Optimization*, *Operational Research, International Journal of Production Research*, and *International Journal of Quality and Reliability Management*. He won the Excellence in Research Award three times and the Excellence in Teaching Award three times from KFUPM. He is the Editor-in-Chief of the *Journal of Quality in Maintenance Engineering*, published by Emerald, U.K..

NABIL DERBEL (Senior Member, IEEE) was born in Sfax, Tunisia, in April 1962. He received the Engineering Diploma degree from École Nationale d'Ingénieurs de Sfax (ENIS), Tunisia, in 1986, the ''Diplôme d'Etudes Approfondies'' degree in automatic control from the Institut National des Sciences Appliquées de Toulouse, France, in 1986, the ''Doctorat d'Université'' degree from the Laboratoire d'Automatique et d'Analyse des Systèmes, Toulouse, France, in 1989, and the ''Doctorat d'État'' degree from École Nationale d'Ingénieurs de Tunis (ENIT), Tunisia. In 1989, he joined Tunis University, where he has been involved in research and education in different positions. Since 2003, he has been a Full Professor in electrical engineering. He is the author and coauthor of more than 90 articles published in international journals and of more than 500 papers published in national and international conferences. His current research interests include optimal control, sliding mode control, sensors, robotic systems, intelligent methods, instrumentation, and renewable energies.